Relating Noninvasive Cardiac Output and Total Peripheral Resistance Estimates to Physical Activity in an Ambulatory Setting

Bryan Haslam*, Ankit Gordhandas*, Catherine Ricciardi†, Thomas Heldt*, George Verghese*

*Computational Physiology and Clinical Inference Group in the Research Laboratory of Electronics
†Clinical Research Center
Massachusetts Institute of Technology
bhaslam@mit.edu

Abstract

The prevalence and cost of heart disease indicate the need for better methods of detecting, diagnosing and treating this pervasive problem. Appropriate monitoring outside of the hospital can potentially lead to earlier diagnosis and reduced costs. We use electrocardiogram (ECG) and continuous arterial blood pressure (ABP) data collected in an ambulatory setting to examine two important cardiovascular quantities, namely cardiac output (CO) and total peripheral resistance (TPR), over a range of physical activities. CO and TPR can be estimated from heart rate, pulse pressure and mean arterial blood pressure, which in turn are directly obtained from the ECG and ABP signals. More specifically, we employ a wearable cardiac and motion monitor designed by colleagues at MIT to simultaneously record ECG and 3-axis acceleration to onboard memory. The acceleration data is used to generate an estimate of physical activity at each time point. Additionally, we use a Portapres continuous blood pressure monitor to concurrently record the ABP waveform. We present representative results from data collected in a controlled ambulatory setting. Heart rate, mean ABP, CO and TPR responses to physical activity are generally consistent with what might be expected from cardiovascular physiology. The longer-term challenge is to correlate the dynamic behavior of these quantities with the state of cardiac health.

Introduction

Background

Heart disease continues to be the leading cause of death in the United States, with 26% of deaths attributed to it (Sebelius, Frieden, and Sondik 2009). Recent estimates put the cost of treatment at $475 billion annually (Lloyd-Jones, Adams, and Brown 2010). The CDC reports that 81 million adults in the United States have cardiovascular disease, and 6 million hospitalizations are attributed to it each year (CDC 2010).

One possibility for reducing costs while maintaining or improving outcomes is more monitoring outside of the hospital. Sensors suitable for ambulatory monitoring have improved rapidly over the last several decades. Commercially

available products include portable or wearable monitors for electrocardiography (ECG), body movement, temperature, pulse oximetry, respiration, blood pressure, and glucose (Brage et al. 2005; Papadopoulos, Crump, and Wilson 2010). With a variety of sensors available, and the promise of more, it is becoming increasingly necessary to demonstrate how such data, collected outside the clinical setting, can be diagnostically useful.

We focus in this paper on ambulatory measurements of ECG, motion, and arterial blood pressure (ABP), and on physiological quantities derived from these measurements.

Essential Cardiovascular Physiology

Entire books are devoted to the exquisite physiology of the cardiovascular system, but we must necessarily make do with the briefest summary.

The electrical activity associated with the contractions and relaxations of cardiac muscle on every heart beat is reflected — in a very distinctive and interpretable way — in features of the ECG signal. These features repeat every heart beat, so heart rate is quite easily determined from the ECG signal. More subtle features of the ECG signal can also be used to diagnose a variety of cardiac conditions.

The pumping heart constitutes a pulsating pressure source that circulates blood through all parts of the body to support metabolism. The average rate of blood volume flowing through the heart is the cardiac output, CO. Various neural, hormonal and metabolic feedback control mechanisms act to maintain blood pressure and flow sufficiently high to allow proper perfusion of body tissues, and to keep CO matched to metabolic needs.

A key neural control mechanism, acting on a time scale of seconds, is the autonomic nervous system, involving action of the sympathetic and parasympathetic nerves. This feedback pathway acts to modulate heart rate, cardiac contractility and the diameter — hence resistance to blood flow — of the arterioles that feed the tissue capillaries. Arteriolar resistance is also regulated by local metabolic needs, allowing the most metabolically active tissues to receive the greatest blood flow. The total peripheral resistance (TPR) is the net resistance to flow seen by the heart, and is the ratio of mean ABP to CO (in close analogy to electrical resistance, which is the ratio of potential difference to current).

Physicians regularly — though often only implicitly —

base clinical decisions on their assessments of the patterns of variation in these related quantities. For instance, a drop in mean ABP without a corresponding drop in CO may prompt the prescription of a (vasopressor) drug to increase TPR and thereby bring mean ABP back to acceptable levels.

Outline

Conventional clinical methods for measuring absolute CO, such as thermodilution or ultrasound, are either invasive or restrictive in methodology, and require expert operators with specialized equipment. Since reliable absolute measurements cannot generally be obtained outside a clinical setting, little has been done to demonstrate how CO and TPR are affected by normal physical activity.

Using ambulatory sensors, we estimate uncalibrated (i.e., relative, not absolute) versions of both quantities over a series of activities, in addition to obtaining an estimate of the concurrent physical activity of the subject. From these three estimates one can hope to eventually make inferences regarding the relative cardiac health of the subject.

The next section (under Methods) describes our data collection setup and the computations used to estimate CO, TPR and physical activity (PA). We then (under Results) describe representative measured data, as well as the CO, TPR and PA waveforms estimated from this data. Specific discussion of these waveforms and their relationships is contained in the same section, while a broader examination of some issues related to ambulatory monitoring is presented in the last section of the paper (as Discussion).

Methods

Data Collection

We collected data from 10 subjects using an experimental wearable ECG/accelerometer device designed by colleagues at MIT, along with a Portapres blood pressure monitoring system to record continuous ABP. The experimental monitor is a low-noise, low-power device that attaches to ECG electrodes placed on the chest; it can record data for up to two weeks, and perform on-board processing of the data using a Texas Instruments TI MSP 430 processor. The accelerometer on the device is an Analog Devices ADXL345.

Wearing these sensors, the subjects were asked to perform specific activities mimicking routine ambulatory activities. These activities included 5 minutes lying down in the supine position, 5 minutes sitting, 5 minutes standing, 1 minute jumping, 1 minute of arm movement, a Valsalva (straining) maneuver, walking and running for 5 minutes each on a treadmill, and stepping for 1 minute. The whole routine was performed twice in succession, with a rest in between, in a total of approximately 1.5 hours per subject.

Estimation

Various models and algorithms have been developed in the literature for estimating CO and TPR from more readily accessible quantities such as heart rate and blood pressure. One simple technique is based on the Windkessel model (Parlikar et al. 2007). In this model, the stroke volume (i.e.,

blood volume ejected by the heart at each beat) is proportional to the pulse pressure, which is the difference between systolic (peak) and diastolic (valley) pressures on the ABP waveform. Since CO is equal to the stroke volume times the heart rate, CO is then proportional to the product of pulse pressure and heart rate. We take this latter product, pulse pressure times heart rate, as our uncalibrated CO estimate. A quantity proportional to TPR can then be estimated by dividing mean ABP by our CO estimate, and this is our uncalibrated TPR estimate. With the ABP waveform data from the Portapres, we have both the pulse pressure and mean pressure of each beat, as required to compute the above estimates.

To estimate the demands on the cardiovascular system, we estimate the physical activity (PA) of the subject using the data from the accelerometer. We calculate the square root of the sum of the variances of all three axes of acceleration, on a sliding four-second window, to obtain an aggregate measure of activity. One limitation of this estimate is that the accelerometer is on the chest, and therefore actually only measures the activity of the torso.
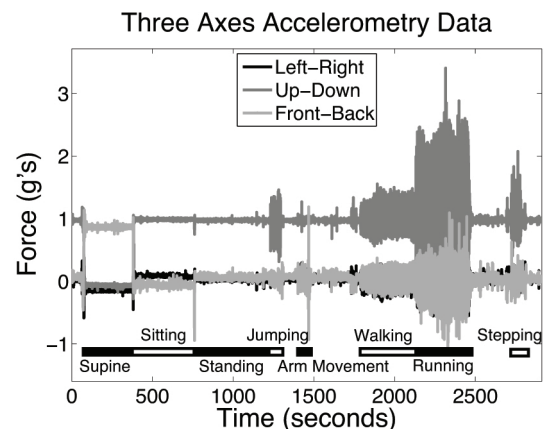
Results

Figure 1: Sample accelerometer data over one entire set of activities for the selected subject. The y-axis is force measured in g's, including gravitational acceleration. Each shade represents a different axis of the accelerometer. Black is the left to right axis parallel to the earth when standing. Dark gray is the top to bottom vertical axis parallel to gravity when standing. Light gray is the front to back axis parallel to gravity when lying on one's back. The activities the subject performs are noted on the bottom of the figure.

Raw Data

Figures 1-3 show the raw data taken from the sensors during testing of a particular subject. Throughout this paper, we present results for only this subject, for whom a relatively noise-free recording was obtained over the entire duration of the test. However, these results are fairly representative of data from other subjects.
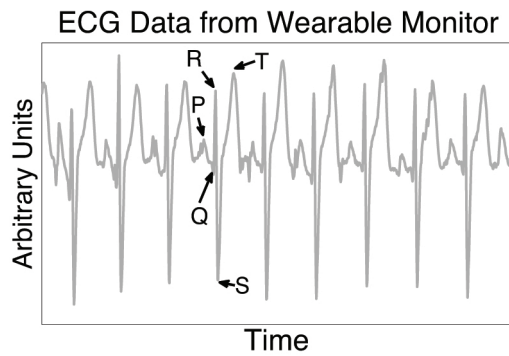
ECG Data from Wearable Monitor

Figure 2: Sample ECG data over a few seconds while the subject was doing light exercise. The P-wave, QRS-complex and T-wave are labeled for one beat.
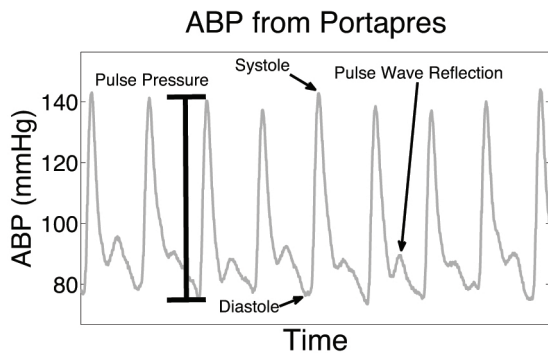
ABP from Portapres

Figure 3: Sample ABP data over a few seconds while the subject was walking on the treadmill. The systolic and diastolic pressures are labeled for one beat. The thick bar represents the pulse pressure (systolic minus diastolic) for that particular beat. A pulse wave reflection is also labeled.

Figure 1 shows the three axes of accelerometry data over the course of one full set of activities; the axes are described in the figure caption. When the subject lies down in the supine position, from an initial standing position at the beginning of the data record, the light gray waveform goes from 0 to 1g, because the associated axis went from being orthogonal to gravity (while the subject stood up) to being parallel to it (once the subject lay down). A subsequent spike in the accelerations shows the transition to sitting. The waveforms during sitting are almost exactly like the standing data that follows, except that the black waveform is slightly higher, probably because the subject was slouching a little when sitting. The jumping activity introduced force most particularly in the vertical direction, and accordingly is picked up by the dark gray waveform that corresponds to this vertical axis. The arm movement resulted in more force on the now-horizontal axis associated with the light gray waveform. The increase in variation of the accelerometer recordings is easily seen when the subject starts walking, and is even more clear when the subject is running. The increased variation reflects more force exerted by the

Heart Rate and Mean ABP
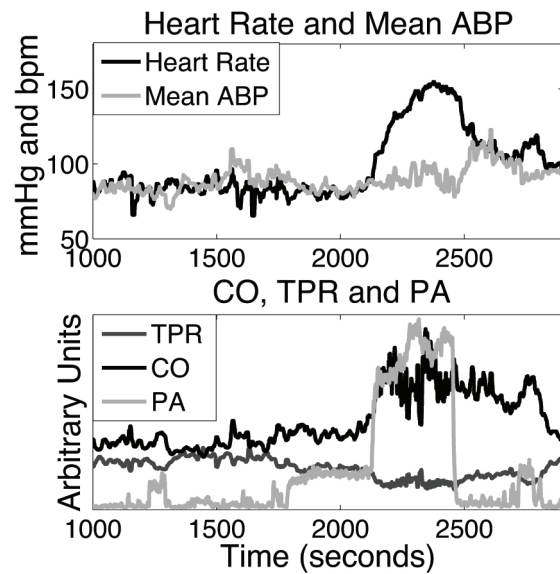

CO, TPR and PA

Figure 4: The top plot shows heart rate (beats per minute) in black, and mean ABP (mmHg) in light gray. The bottom plot shows our (uncalibrated) CO estimate in black, the associated (uncalibrated) TPR estimate in dark gray, and PA in light gray, all without units. The estimates in the bottom plot are based in part on the data shown in the top plot. Both plots are on the same time scale.

body.

Figure 2 shows raw ECG data that was collected from the experimental wearable device. There is some noticeable high-frequency noise, probably due to muscle activity under the electrodes; some low-frequency variation is also visible, probably associated with movement of the electrodes due to respiration. The R-wave is clearly distinguishable, and "instantaneous" heart rate can be calculated easily from the reciprocal of the interval between R-waves (the RR interval).

Figure 3 shows raw ABP data collected from the Finapres while the subject was walking on the treadmill. The shape of each beat is typical for an ABP waveform measurement. The height of the sharp rise from diastole to systole is the pulse pressure; the small bump after each systole is the reflected pressure wave that travels back towards the heart from the first major discontinuity in the arterial path. Some noise is present, as indicated by the inconsistency of the reflected pressure wave; this is likely a result of the subject walking. Again, even in the presence of noise, it is easy to extract the mean ABP and pulse pressure from the waveform.

Estimated CO, TPR and PA

The estimated values for CO, TPR and PA are plotted in Figures 4 and 5, along with the values for heart rate and mean ABP which were used for the estimation. In this subsection we will point out some of the interesting features of these plots, and relate them to the underlying physiology.

Figure 4 shows an approximately 30-minute section of data which included the most physical activity. When the

subject begins jumping, noted by the sharp rise in PA around 1200 seconds, the CO rises and the TPR falls gradually. After the subject stops, noted by the sharp fall in PA, the CO quickly falls and the TPR rises more gradually. It appears that both do not just return to baseline, but overshoot it slightly. The heart rate does not appear to react strongly to this light activity, but it is evident that the mean ABP drops after the exercise stops.

At around 1750 seconds the subject gets on the treadmill, but does not start walking consistently until about 1800 seconds. From 1750 seconds on there is again a gradual increase in CO and gradual fall in TPR, though both level off. When the subject begins to run on the treadmill around 2150 seconds, the CO rises much more significantly, reflecting the increased metabolic demand. The TPR also falls much more quickly, largely reflecting dilation of arterioles in the muscles under local metabolic control, to increase blood flow there. The heart rate rises more gradually than CO and peaks several minutes into the exercise. It can be seen that the ABP also rises somewhat, further enhancing perfusion to the muscles. The CO and TPR are fairly noisy during this stretch, probably due to the motion of the sensors during running. Immediately after the subject stops running, heart rate drops significantly, the CO drops by a small amount but stays relatively elevated, the TPR rises very gradually, and ABP shows a sharper rise. The interpretation of these post-running transients is more subtle, as it involves the interaction of several mechanisms (Costanzo 2010; Froelicher and Myers 2006).

At 2700 seconds the subject begins simulated stair climbing by stepping on and off the back of the treadmill. Though the exercise appears to require a similar level of PA as the jumping and walking, there is a larger increase in CO and a sharper decrease in TPR than noted in those activities. Afterwards CO falls quickly and TPR rises close to the initial baseline.

Figure 5 is a zoomed out look of the same data, showing one whole set of activities and the start of the next set, plotted over a window of approximately 75 minutes. The sharp spikes in PA are the transitions, such as lying down or standing up, between different positions. They require energy themselves, but the specific transition also is important context. For example, after the first spike, the CO drops and in the top plot it can be seen that the heart rate and mean ABP have dropped significantly. Referring back to Figure 1, this corresponds to lying down, at which point the need for high mean ABP to work against gravity is reduced.

Clearly much remains to be understood about the physiological responses, and what they tell us about the subject's health, in even relatively simple ambulatory settings, such as those used in our experiments.

Discussion

Many challenges are presented in an outpatient monitoring paradigm. An immediate one is noise and artifact. Physicians are used to monitoring vital signs in a very controlled environment, where a patient is likely inactive or following the specific protocol of a stress test, under close supervision. Two approaches to improving robustness to noise and
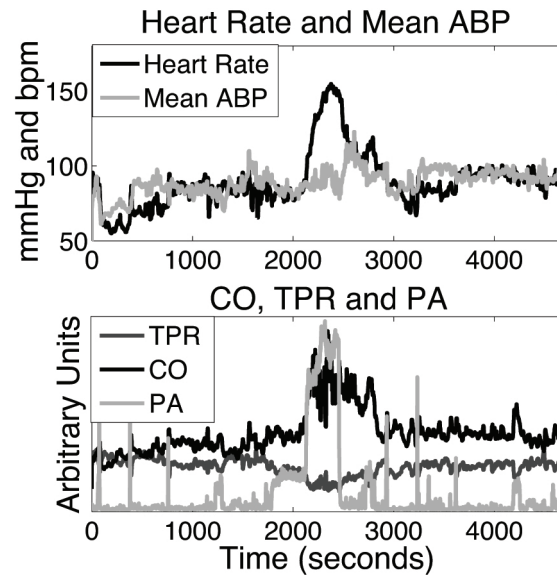

Figure 5: The two plots here follow the same format as Figure 4 but show more data before and after.

artifact are better sensors and more accurate algorithms, including algorithms for signal quality assessment. Even with such improvements, it is unlikely that ambulatory monitoring will ever have noise levels as low as monitoring in a hospital setting.

Another challenge is the volume of data. Current sensors allow us to easily record the ECG morphology of every heart beat for many days, leading to a data record that can no longer be inspected personally by a cardiologist. As new sensors allow for simultaneously monitoring other quantities, such as blood pressure, new ways of analyzing and presenting the data will have to be explored to make the data useful. For example, clinicians usually take blood pressure once during a visit, so the pulse pressure and mean pressure for each of the approximately 100,000 heart beats in a day might be of no immediate use for them. In our ambulatory testing, we used known physiology to transform the large volume of data into estimates of important and clinically actionable physiological quantities that are more informative to track.

A third challenge is that of alarms and alerts, which are the current usage model for most monitoring. The idea is to use them for finding problems and warning clinicians. However, clinicians often end up ignoring them due to a high false positive rate. To be effective, a monitor needs to catch a problem before it gets out of control, and then the problem must be effectively communicated to a physician.

Related to alerts is the issue of scoring for risk stratification. In research settings, many heart health scores have been proposed for risk stratification. Examples include maximum exercise capacity, heart rate variability (HRV), heart rate recovery (HRR), and morphological variability (Malik and Camm 1990; Cole et al. 1999; Myers et al. 2002; Syed et al. 2009). Strong correlations have been demon-

strated with mortality in these cases, but the underlying mechanisms are generally still not well understood. The prevailing theory is that HRV and HRR can be used to estimate the performance of the autonomic response system (Schwartz and Ferrari 2010). Though HRV has been studied for decades and has promise, it has not found its way into the clinic. By reporting to physicians quantities that they are familiar working with, they are much more likely to incorporate that data into their practice.

Conclusions

Up to this point wearable sensors have not made their way into everyday medicine, but have vast potential. We have presented results showing the possibility of estimating important quantities such as CO, TPR, and PA from data collected with wearable and portable sensors. Though not free of noise, the data shows clear patterns that can be explained by the underlying cardiovascular physiology. By using known physiology, we leverage the data we collect from wearable sensors and produce estimates that can be clinically relevant. We recognize the need for further development in several areas of this research.

Acknowledgements

References

Brage, S.; Brage, N.; Franks, P.; Ekelund, U.; and Wareham, N. J. 2005. Reliability and validity of the combined heart rate and movement sensor actiheart. *European Journal of Clinical Nutrition* 59:561–570.

CDC. 2010. Addressing the nation's leading killers: At a glance. Heart disease and stroke prevention, Centers for Disease Control and Prevention, Atlanta, GA.

Cole, C.; Blackstone, E.; Pashkow, F.; Snader, C.; and Lauer, M. 1999. Heart-rate recovery immediately after exercise as a predictor of mortality. *New England Journal of Medicine* 341:1351–1357.

Costanzo, L. 2010. *Physiology*. Elsevier, 4th edition.

Froelicher, V., and Myers, J. 2006. *Exercise and the Heart*. Elsevier, 5th edition.

Lloyd-Jones, D.; Adams, R. J.; and Brown, T. M. 2010. Heart disease and stroke statistics-2010 uptdate. *Circulation* 121:e46–e215.

Malik, M., and Camm, A. 1990. Heart rate variability. *Clinical Cardiology* 13(8):570–576.

Myers, J.; Prakash, M.; Froelicher, V.; Do, D.; Partington, S.; and Atwood, J. E. 2002. Exercise capacity and mortality among men referred for exercise testing. *New England Journal of Medicine* 346:793–801.

Papadopoulos, A.; Crump, C.; and Wilson, B. 2010. Comprehensive home monitoring system for the elderly. In *WH '10 Wireless Health 2010*, doi:10.1145/1921081.1921118. ACM.

Parlikar, T.; Heldt, T.; Ranade, G.; and Verghese, G. 2007. Model-based estimation of cardiac output and total peripheral resistance. *Computers in Cardiology* 34:379–382.

Schwartz, P. J., and Ferrari, G. M. D. 2010. Sympathetic-parasympathetic interaction in health and disease: abnormalities and relevance in heart failure. *Heart Failure Review* doi: 10.1007/s10741–010–9179–1.

Sebelius, K.; Frieden, T.; and Sondik, E. 2009. Health, united states, 2009. National vital statistics report, National Center for Health Statistics, Hyattsville, MD.

Syed, Z.; Scirica, B.; Mohanavelu, S.; Sung, P.; Michelson, E.; Cannon, C.; Stone, P.; Stultz, C.; and Guttag, J. 2009. Relation of death within 90 days of non-st-elevation acute coronary syndromes to variability in electrocardiographic morphology. *American Journal of Cardiology* 103(3):307–311.